POLYPUBLIE
Polytechnique Montréal

POLYTECHNIQUE MONTRÉAL
UNIVERSITÉ D'INGÉNIERIE

Titre: Title:	Flexible organic ion-gated transistors with low operating voltage and light-sensing application
Auteurs: Authors:	Mona Azimi, Arunprabaharan Subramanian, Nur Adilah Roslan, & Fabio Cicoira
Date:	2021
Type:	Article de revue / Article
Référence: Citation:	Azimi, M., Subramanian, A., Roslan, N. A., & Cicoira, F. (2021). Flexible organic ion-gated transistors with low operating voltage and light-sensing application. Journal of Physics: Materials, 4(2), 024001 (11 pages). https://doi.org/10.1088/2515-7639/abd018

Document en libre accès dans PolyPublie
Open Access document in PolyPublie

URL de PolyPublie: PolyPublie URL:	https://publications.polymtl.ca/9316/
Version:	Version officielle de l'éditeur / Published version Révisé par les pairs / Refereed
Conditions d'utilisation: Terms of Use:	CC BY

Document publié chez l'éditeur officiel
Document issued by the official publisher

Titre de la revue: Journal Title:	Journal of Physics: Materials (vol. 4, no. 2)
Maison d'édition: Publisher:	IOP Publishing
URL officiel: Official URL:	https://doi.org/10.1088/2515-7639/abd018
Mention légale: Legal notice:	

PAPER • OPEN ACCESS

Flexible organic ion-gated transistors with low operating voltage and light-sensing application

To cite this article: Mona Azimi *et al* 2021 *J. Phys. Mater.* **4** 024001

View the article online for updates and enhancements.

Journal of Physics: Materials

PAPER

Flexible organic ion-gated transistors with low operating voltage and light-sensing application

Mona Azimi[1], Arunprabaharan Subramanian[1], Nur Adilah Roslan[2] and Fabio Cicoira[1]

[1] Department of Chemical Engineering, Polytechnique Montréal, Montreal, Quebec H3T 1J4, Canada
[2] Department of Physics, Faculty of Science, University Putra Malaysia, 43400 UPM Serdang, Selangor Darul Ehsan, Malaysia

E-mail: fabio.cicoira@polymtl.ca

Abstract

Ion-gated transistors are attracting significant attention due to their low operating voltage (<1 V) and modulation of charge carrier density by ion-gating media. Here we report flexible organic ion-gated transistors based on the high mobility donor–acceptor conjugated copolymer poly[4-(4,4-dihexadecyl 4H-cyclopenta[1,2-b:5,4-b′]-dithiophen-2-yl)-alt[1,2,5]thiadiazolo[3,4c]pyridine](PCDTPT) and the ionic liquid [1-ethyl-3 methylimidazolium bis(trifluoromethylsulfonyl)imide] as the ion-gating medium. Electrical characteristics of devices made on both [rigid (SiO_2/Si) and flexible (polyimide (PI))] substrates showed very similar values of hole mobility (~ 1 cm^2 V^{-1} s^{-1}) and ON–OFF ratio ($\sim 10^5$). Flexible ion-gated transistors showed good mechanical stability at different bending curvature radii and under repetitive bending cycles. The mobility of flexible ion-gated transistors remained almost unchanged upon bending. After 1000 bending cycles the mobility decreased by 20% of its initial value. Flexible photodetectors based on PCDTPT ion-gated transistors showed photosensitivity and photoresponsivity values of 0.4 and 93 AW^{-1}.

1. Introduction

Flexible organic electronic devices have aroused a great deal of interest for various novel applications, including wearable devices, flexible displays and sensor systems, due to light weight, ability to withstand mechanical deformation, printability, ease of processing and easy skin attachment (Yuvaraja *et al* 2020). Organic thin film transistors are considered as the essential building blocks of electronic systems. Conjugated organic semiconductors have been extensively explored as active materials in flexible devices due to their low temperature processing, tunable energy levels, charge transport properties, and compatibility with fabrication processes over large areas, such as roll-to-roll, screen and inkjet printing (Kim *et al* 2017, Sadeghi *et al* 2020). Polymer substrates such as polyimide (PI) polytetrafluoroethylene, polyethylene terephthalate, and polyethylene naphthalate are the most commonly utilized for flexible electronics (Gao *et al* 2019). Ion-gated organic transistors are a category of devices with low operating voltage (<1 V), where charge carrier density in the active material is modulated by exploiting an ionic gating medium, which is in direct contact with the channel material. Metal oxides as well as organic conjugated semiconductors, are being exploited as active materials for ion-gated transistors (Valitova *et al* 2016, 2017, Xu *et al* 2017b, Balakrishna Pillai *et al* 2018, Silva *et al* 2019, Lan *et al* 2019, Zhu *et al* 2019, Yan *et al* 2019, Meng *et al* 2020, Son *et al* 2020, Subramanian *et al* 2020 Zare Bidoky *et al* 2020). The use of ionic gating media, instead of brittle oxide-based dielectrics, e.g. silicon, aluminum or hafnium oxides, is attractive for the fabrication of high-performance flexible transistors.

Organic phototransistors encompass light detection, light switching and signal amplification in a single device and typically show higher photosensitivity and lower noise current with respect to organic photodiodes, due the presence of the gate electrode that amplifies the photogenerated electrical signal
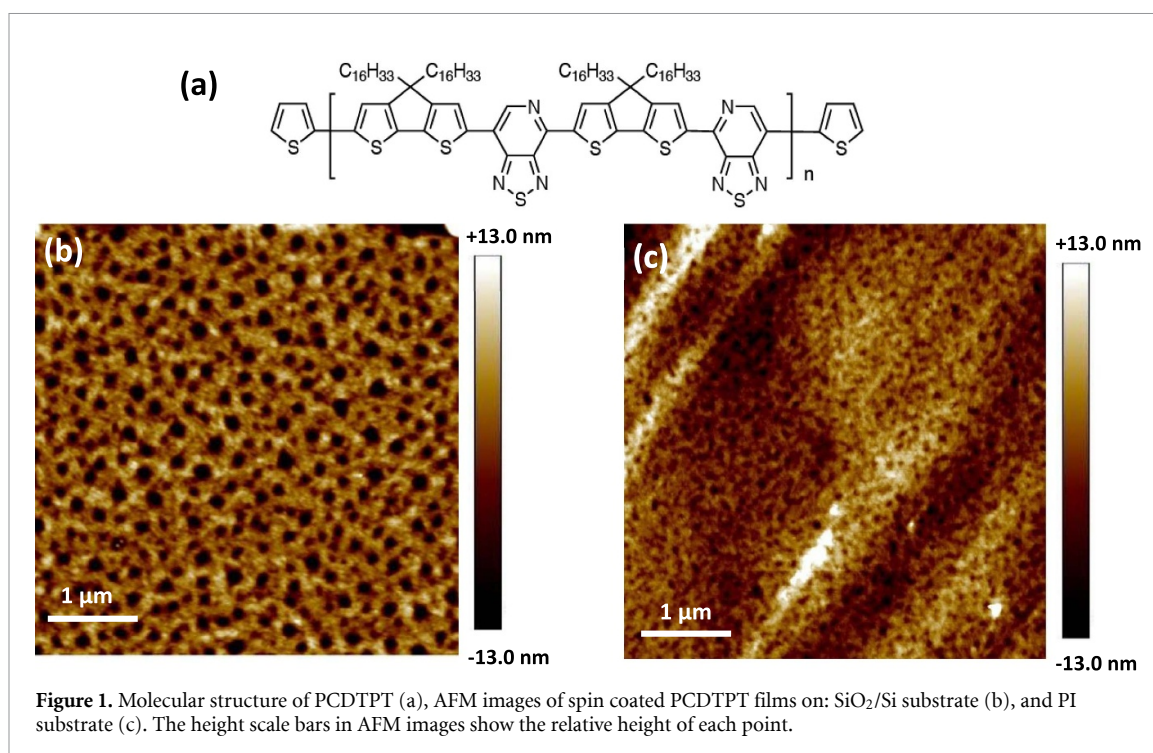
Figure 1. Molecular structure of PCDTPT (a), AFM images of spin coated PCDTPT films on: SiO₂/Si substrate (b), and PI substrate (c). The height scale bars in AFM images show the relative height of each point.

(Nam *et al* 2014, Zhang *et al* 2017b). Light absorption by the semiconductor layer leads to the generation of excitons with a binding energy of a few 100 meV, which are dissociated into free charges by the applied electric field and detected as an increase in source-drain current. The flux of free charges in the semiconductor layer is correlated with the intensity and wavelength of the absorbed light (Lamport *et al* 2018). Conformable phototransistors are attractive for applications in curved image sensors, which are a crucial components in bio-inspired imaging systems, artificial compound eyes and artificial retinas (Kim *et al* 2014, Huang *et al* 2017, Xu *et al* 2017a). One of the drawbacks of organic phototransistors is their high driving voltage (typically higher than 20 V), which leads to high energy consumption (Wang *et al* 2018). Making use of low-voltage ion-gated transistors is a feasible way to effectively reduce energy consumption (Guo *et al* 2019). In addition to the low operating voltage of ion-gated transistors and modulation of charge carrier density by ion-gating media they have merits including flexibility, printability and bio-sensing applications (Kergoat *et al* 2012).

In recent years, several donor–acceptor conjugated semiconductors with narrow band gap and high mobility have been synthesized (Kim *et al* 2019). Intermolecular charge transfer in these materials leads to very narrow band gaps, which improve the harvest of incident photons. Furthermore, strong $\pi-\pi$ stacking causes high charge carrier mobility. Therefore, single-component donor–acceptor conjugated semiconductors as substitutes for bulk heterojunctions (BHJs) and bilayer systems are of great significance (Wang *et al* 2020). Poly[4-(4,4-dihexadecyl4H-cyclopenta[1,2-b:5,4-b′]-dithiophen-2-yl) alt[1,2,5]thiadiazolo[3,4c]pyridine](PCDTPT) is a donor–acceptor conjugated copolymer with a cyclopenta[2,1-b:3,4-b′]dithiophene (CDT) donor unit, and a [1,2,5]thiadiazolo[3,4c]pyridine (PT) acceptor unit (figure 1(a)). Lowest unoccupied molecular orbital and highest occupied molecular orbital of PCDTPT are −3.7 eV and −5.16 eV, respectively. Strong electronic delocalization between donor and acceptor units enhances charge transport along the PCDTPT chain. Several p-type field effect transistors (FETs) based on this material have been reported, whose mobilities have been typically extracted at high negative drain-source (V_{ds}) and gate-source (V_{gs}) voltages (−40 V or higher). The reported hole mobilities for FETs based on PCDTPT with bottom gate-top contact configuration on SiO₂ treated with octyltrichlorosilane (OTS8) are ∼0.6 cm² V⁻¹ s⁻¹ (Ying *et al* 2011). Drop-casted PCDTPT on nano-grooved SiO₂ led to mobilities of ∼20 cm² V⁻¹ s⁻¹ (Tseng *et al* 2014), whereas slot-die coating on similar substrates led to mobilities of ∼5 cm² V⁻¹ s⁻¹ (Kyaw *et al* 2016). PCDTPT based OFETs, with a bottom gate bottom contact configuration and a nano-grooved polymer dielectric (poly(4-vinylphenol)) cross-linked with 4,4′-(hexafluoroisopropylidene)-diphthalic anhydride (PVP:HDA) exhibited a mobility of ∼20 cm² V⁻¹ s⁻¹ on rigid and 10.5 cm² V⁻¹ s⁻¹ on flexible substrates (Lee *et al* 2016). FETs based on single-crystal PCDTPT nanowires showed a mobility of ∼70 cm² V⁻¹ s⁻¹ (Park *et al* 2019). Photo-sensing ability of PCDTPT has been shown for a multilevel optical memory, using a mixture of CdSe/ZnS quantum dots and poly

(methyl methacrylate) (PMMA) as floating gate electrode with vertical and planar configuration. The vertical devices, operated at -40 V, showed a photoresponsivity of 104 AW^{-1} and a photosensitivity 200, which are significantly higher than the values of a planar device (Wu *et al* 2019). This improvement is related to the very short channel length (tens of nanometers), which leads to an easier dissociation of photogenerated excitons. Photoresponsivity of the blend PCDTPT: [6,6]-phenyl C61-butyric acid methyl ester (PCBM) (BHJ) showed an improvement with respect to pure PCDTPT both for planar and vertical configurations. (Zhang *et al* 2019).

Here, we demonstrate PCDTPT flexible ion-gated transistors using PI as a substrate. PI has good chemical and thermal stability, making it an appropriate candidate for flexible devices. PCDTPT is a solution processable material with remarkably high hole mobility. [1-ethyl-3 methylimidazolium bis (trifluoromethylsulfonyl) imide] ([EMIM][TFSI]) was used as gating medium as it has good stability and wide electrochemical window. Charge carrier mobilities of $\sim$0.9 cm^2 V^{-1} s^{-1} and ON–OFF ratios of $\sim$10^5 were obtained for devices on rigid (SiO$_2$/Si) and flexible substrates. Electrical characteristics of flexible devices under different bending radii and several bending cycles showed good mechanical flexibility. We used these devices as phototransistors based on PCDTPT, which showed a photosensitivity of 0.4 and a photoresponsivity of 93 AW^{-1} at $V_g = -1$ V.

2. Experimental

2.1. Materials

PCDTPT ($M_w = 50$KDa, PDI = 2) was purchased from 1-Material-Organic Nano Electronic and chloroform (CHCl$_3$) was purchased from Acros Organics. The ionic liquid ([EMIM][TFSI]) with viscosity of 39.4 mPa·s and ionic conductivity of 6.63 mS cm^{-1} was supplied by IoLiTec and purified under vacuum ($\sim$10^{-5} Torr) at 60 °C for 24 h before use. PI sheets (PolyFLE™ XF-102) with a thickness of 125 μm were purchased from Polyonics. Polydimethylsiloxane (PDMS) (SYLGARD™ 184) was supplied by Dow Chemical Company. Carbon paper (Spectracarb 2050), activated carbon (Norit CA1, Sigma-Aldrich, 28 mg ml^{-1}), polyvinylidene fluoride (PVDF) (Kynar HSV900), and N-methyl pyrrolidone (NMP) (Fluka, >99.0%) were used for gate electrode fabrication.

2.2. Device fabrication

Activated carbon was chosen as gate electrode since its high surface area enables transistors to modulate current efficiently. In order to prepare gate electrodes, carbon paper (6×3 mm^2) was immersed in a solution of activated carbon (28 mg ml^{-1}) and PVDF (1.4 mg ml^{-1}) in NMP. Carbon paper pieces coated with activated carbon ink were heated at 60 °C for 5 h to remove solvent. The detailed procedure for the preparation of activated carbon electrodes has been described elsewhere (Tang *et al* 2015). Source and drain electrodes (channel width/length (W/L) = 4000 μm/10 μm) were patterned on SiO$_2$/Si substrate by photolithography and lift-off. For photolithography on SiO$_2$/Si substrate, a positive tone photoresist (AZ900) was spin-coated on substrates at 3000 rpm for 1 min. Samples were soft baked (at 90 °C for 1.5 min) and exposed to UV light through a photo mask in a Karl Suss mask aligner (MA-6). Next, a post-exposure bake was carried out at 115 °C for 1.5 min and the photoresist was developed in AZ-726 (MicroChem) developer for 60 s. Finally, samples were rinsed with deionized water several times in order to remove excess developer and dried with a N$_2$ flow. After metal deposition (40 nm gold and 5 nm titanium as adhesion layer), samples were immersed in PG remover to strip out the photoresist and sonicated in isopropyl alcohol (IPA), acetone, and IPA for 5, 10, and 5 min sequentially. For photolithography on flexible substrates, PI sheets were cleaned by ultrasonication in acetone, IPA, and deionized (DI) water for 10 min each. A thin PDMS (elastomer/curing agent (10:1 wt.%)) layer was spin coated (500 rpm for 30 s) on glass slides and heated at 100 °C for 15 min. Then PI sheets (75 mm $\times$ 50 mm) were laminated on the semi-cured PDMS layer and heated at 100 °C for 15 min. This step was performed to ensure a flat surface during photolithography (Zhang *et al* 2017a). The following steps were performed as described for the rigid substrates.

PCDTPT solution (2.5 mg ml^{-1}) in CHCl$_3$ was prepared and stirred overnight. Next, PCDTPT films were deposited on prepatterned substrates inside a glovebox (<5 ppm O$_2$, H$_2$O) by spin coating at 1000 rpm for 1 min and then heated at 200 °C for 10 min on a hotplate.

[EMIM][TFSI] was dropped on PVDF hydrophobic membrane (Durapore GVHP 01300 with a pore size of 0.22 μm, 9×4 mm^2). The color of the membrane changed from white to transparent by absorbing ionic liquid, then the membrane containing ionic liquid was placed on PCDTPT film. We used PVDF membrane soaked with ionic liquid for constructing ionic gating media in order to prevent leakage of ionic liquid for the application in a flexible device. The activated carbon electrode was placed on top of the PVDF membrane for the transistor devices (figure S1 (available online at stacks.iop.org/JPMATER/4/024001/mmedia)) (Valitova *et al* 2016), whereas it was placed in a position not covering the channel for the phototransistor (figure 6(a)).
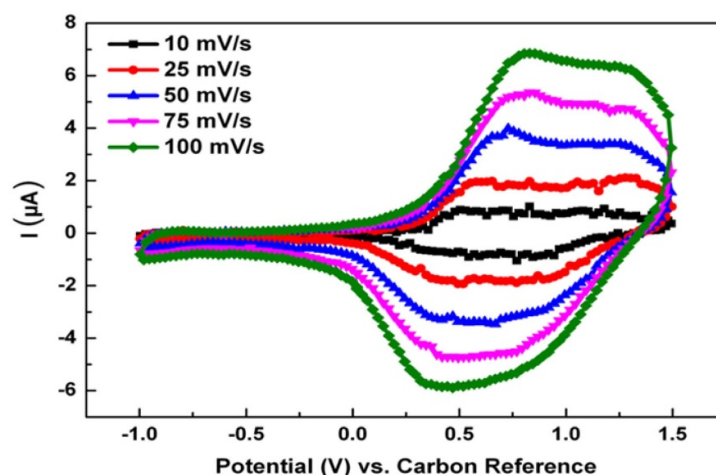
Figure 2. Cyclic voltammetry of PCDTPT films in transistor configuration at different scan rates. [EMIM][TFSI] acts as electrolyte, activated carbon coated carbon paper as counter and quasi-reference electrode, and PCDTPT film as working electrode.

2.3. Characterization

Atomic force microscopy (AFM) images were taken in ambient conditions with a Digital Instruments Dimension 3100 equipped with etched silicon cantilevers (ACTA from Applied NanoStructures, Inc.) with a resonance frequency of 300 kHz, a spring constant of 40 N m^{-1}, and a tip radius <10 nm. Imaging was performed in tapping mode and scan rate of 1 Hz and images were analyzed by Nanoscope software. Cyclic voltammetry was performed with a VERSASTAT 4 (Princeton Applied Research) potentiostat under N$_2$ in a glovebox. The experimental condition was a two-electrode configuration such that the PCDTPT film in channel area acted as the working electrode and an activated carbon gate electrode (with high surface area and specific capacitance of about 100 F g^{-1}) acted as counter and quasi-reference electrode. Transistor characterizations were conducted by semiconductor parameter analyzer (Agilent B1500A) and electrical probe station in a glovebox. We performed characterization of three devices in the same conditions. Optoelectronic measurements were performed at room temperature in a cryostat probe station (P $\sim 10^{-4}$ Torr). A solar simulator (SLB-300A Compact Solar Simulator Class AAA) with a light power of 100 mWcm^{-2} and wavelength range of 400 nm–1100 nm was used to evaluate the device characteristics under illumination, under a vacuum of $\sim 10^{-4}$ Torr. The devices were fabricated in the glovebox and briefly exposed to air to be transferred to the vacuum chamber of the solar simulator. Ultraviolet/Visible (UV/Vis) absorption spectra were measured with a PerkinElmer Lambda 9 UV/VIS/NIR Spectrophotometer for thin films of PCDTPT, spin-coated (1000 rpm, 1 min) on fused silica.

3. Results and discussion

AFM images (figure 1(b)) show that PCDTPT films on SiO$_2$/Si have a porous structure, which can be explained by the rapid evaporation of the processing solvent (chloroform), upon heating at 200 °C, due to its low boiling point (61.2 °C). The presence of the pores favors an effective contact of the ionic liquid with the semiconductor film during ion gating (Tartakovsky and Dentz 2019). Films on PI substrates show pores smaller than that of SiO$_2$/Si, likely because of the greater affinity of PCDTPT to hydrophobic substrates (Williams and Goodman 1974, Soon *et al* 2013). The root mean square (rms) surface roughness of the PCDTPT films is ∼11 nm on SiO$_2$/Si and ∼7 nm on PI.

In order to obtain the electrochemical characteristic of PCDTPT film in transistor configuration, we performed cyclic voltammetry at different scan rates (figure 2). In the ion-gated transistors, the polymeric channel material typically shows an electrochemical (redox) activity. By performing CV before transistor characterization, it is possible to verify the presence of redox reactions and to identify the voltage stability window of the devices. The electrochemical activity of PCDTPT starts at ca. 0.5 V versus activated carbon reference and the safe operational voltage for transistors is between ca. 0.2 V and −1.5 V. No significant redox reactions were observed in the range of 0 V to −1 V. For forward scan, a broad anodic peak in the interval of 0 V–1.5 V was observed at all scan rates and it became more significant at higher scan rates. In the backward scan, a cathodic peak with a slightly negative shift compared to the anodic peak was observed in the voltage range of 1 V–0.25 V. The current increases upon increasing the scan rate and the peak currents
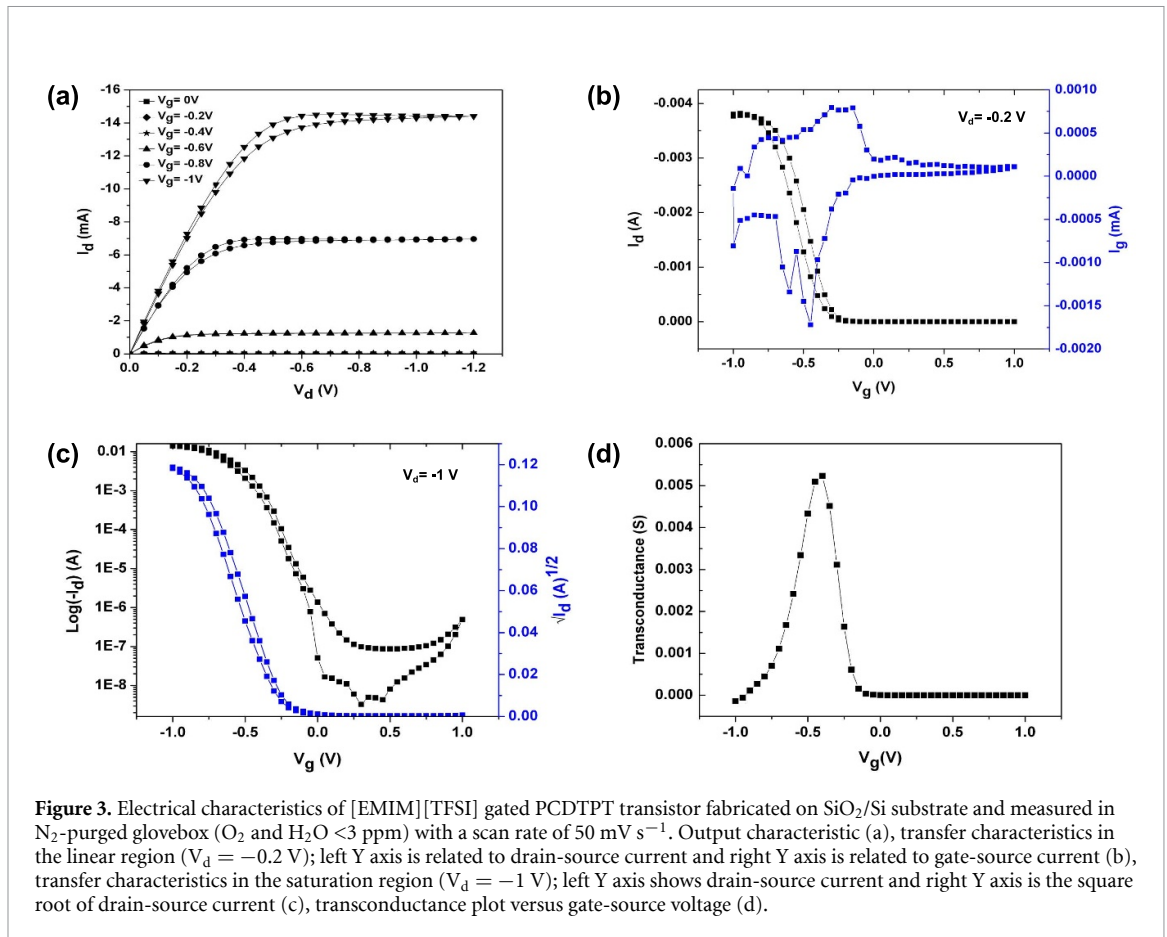
Figure 3. Electrical characteristics of [EMIM][TFSI] gated PCDTPT transistor fabricated on SiO_2/Si substrate and measured in N_2-purged glovebox (O_2 and H_2O <3 ppm) with a scan rate of 50 mV s^{-1}. Output characteristic (a), transfer characteristics in the linear region ($V_d = -0.2$ V); left Y axis is related to drain-source current and right Y axis is related to gate-source current (b), transfer characteristics in the saturation region ($V_d = -1$ V); left Y axis shows drain-source current and right Y axis is the square root of drain-source current (c), transconductance plot versus gate-source voltage (d).

are linearly dependent on the square root of the potential (figure S2), which indicates a diffusion-limited response (Elgrishi *et al* 2018). Since there is a linear dependence between peak current versus scan rate, the electrochemical processes in PCDTPT are (pseudo)capacitive (Allen and Larry 2001). Overall, these results show that PCDTPT is electrochemically active in the presence of [EMIM][TFSI] ionic liquid and undergoes doping and de-doping reactions.

PCDTPT ion-gated transistors on rigid and flexible substrates are capable of operating in enhancement mode at low voltage (<1.2 V) and show typical p-type characteristics. Output and transfer characteristics of ion-gated transistors on SiO_2/Si substrate are presented in figures 3(a) and (c). Hysteresis effects, mostly due to the slow motion of ions during doping and de-doping of the PCDTPT films, are not significant at sweeping rates of 50 mV s^{-1} and 100 mV s^{-1}, whereas they are observed at 10 mV s^{-1} (figure S4). At lower scan rates, during forward bias ions have sufficient time to penetrate in the polymer film, so a longer time will be needed for them to be released back to the gating medium during backward biasing, which results in larger hysteresis (Meng *et al* 2015).

The charge carrier mobility is extracted from $\mu = \frac{L}{W} \frac{I_d}{V_d p e}$, where L is the channel length (10 μm) and w the channel width (4000 μm), I_d is the drain-source current, V_d is the drain-source voltage and p the charge carrier density (Xia *et al* 2009). The charge density (p) was obtained from $= \frac{Q}{eA} = \frac{\int I_g dV_g}{r_v eA}$, where Q is the total accumulated charge, which can be calculated by integration of the gate current (I_g) versus V_g (figure 3(b), blue graph), A is the area of the interface between the active layer and the ionic liquid (4 mm × 9 mm), r_v is the scan rate of V_g and e is the elementary charge. We obtained a charge carrier density of $\sim 2 \times 10^{14}$ cm^{-2}, which led to a mobility of 1.00 ± 0.10 cm^2 V^{-1} s^{-1} (the error represents the standard deviation of the mobility values of six devices (transistor characteristics of two more devices are shown in figure S3)). The ON–OFF ratio was $\sim 10^5$. The transconductance, i.e. the derivative of drain current (I_d) versus gate voltage (V_g), showed a maximum of 5 mS at $V_g = -0.45$ V (figure 3(d)). This value is among the highest previously reported values for organic semiconductor based, e.g. (poly(3-hexylthiophene) (P3HT)) ion gated transistor devices (Cho *et al* 2008, Braga *et al* 2012). We correlate the high value of transconductance with the effective penetration of ions in the porous films (Sun *et al* 2018) .

We also evaluated the device characteristics in ambient air. The devices were assembled inside the glovebox and transferred to ambient condition. Electrical characterization of devices after 30 min in ambient
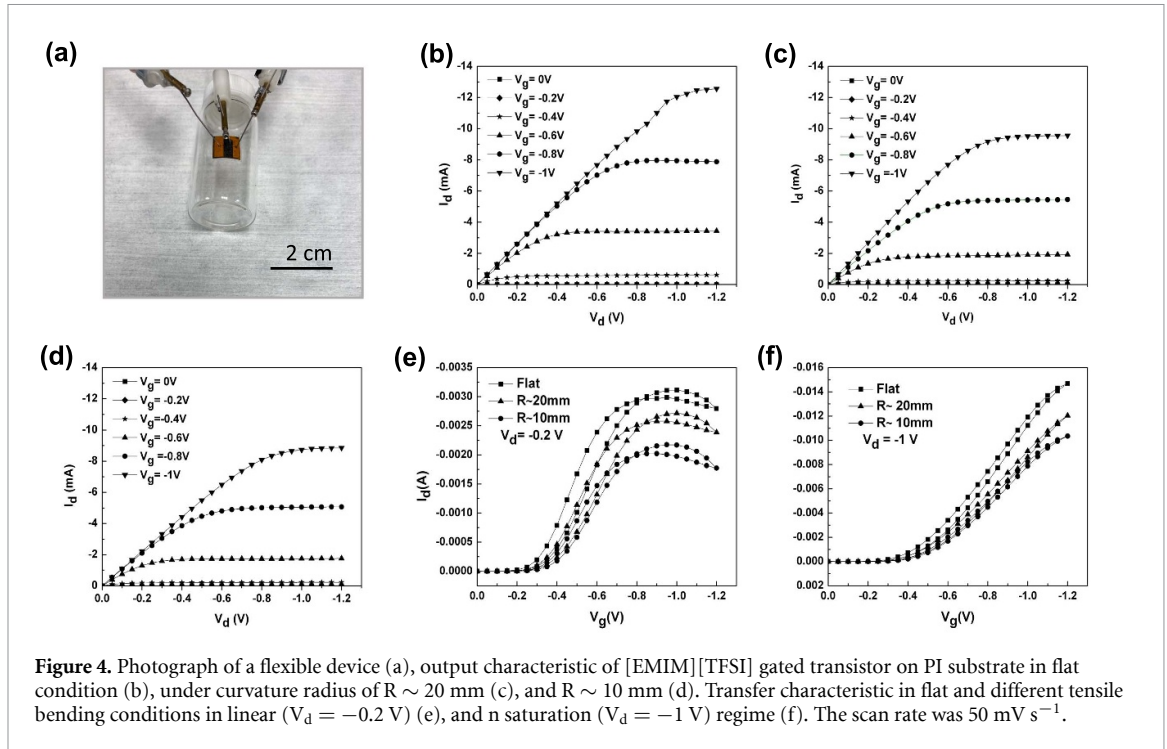
Figure 4. Photograph of a flexible device (a), output characteristic of [EMIM][TFSI] gated transistor on PI substrate in flat condition (b), under curvature radius of R ∼ 20 mm (c), and R ∼ 10 mm (d). Transfer characteristic in flat and different tensile bending conditions in linear ($V_d = -0.2$ V) (e), and n saturation ($V_d = -1$ V) regime (f). The scan rate was 50 mV s^{-1}.
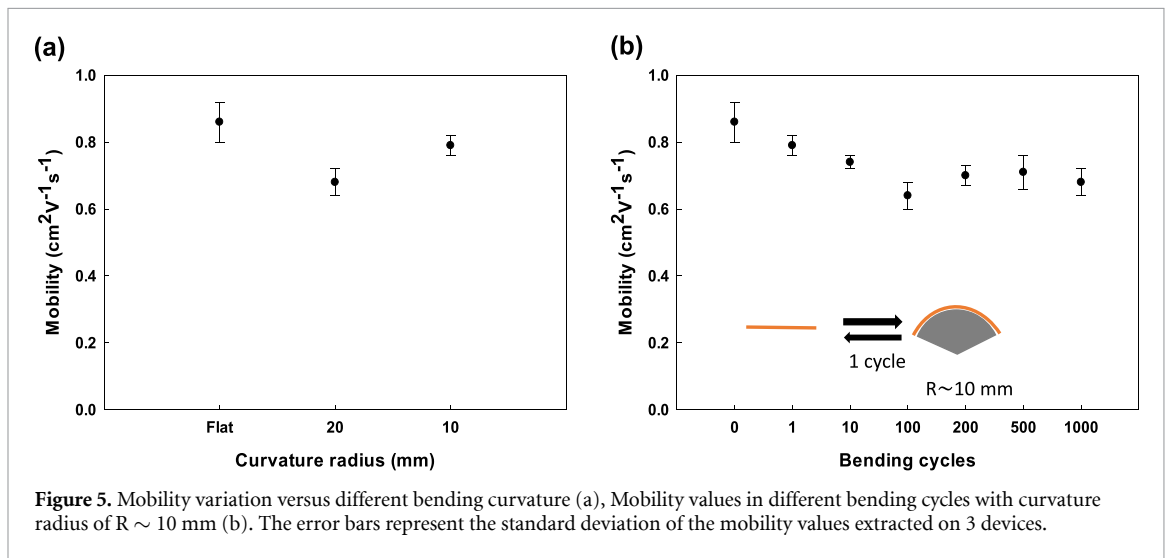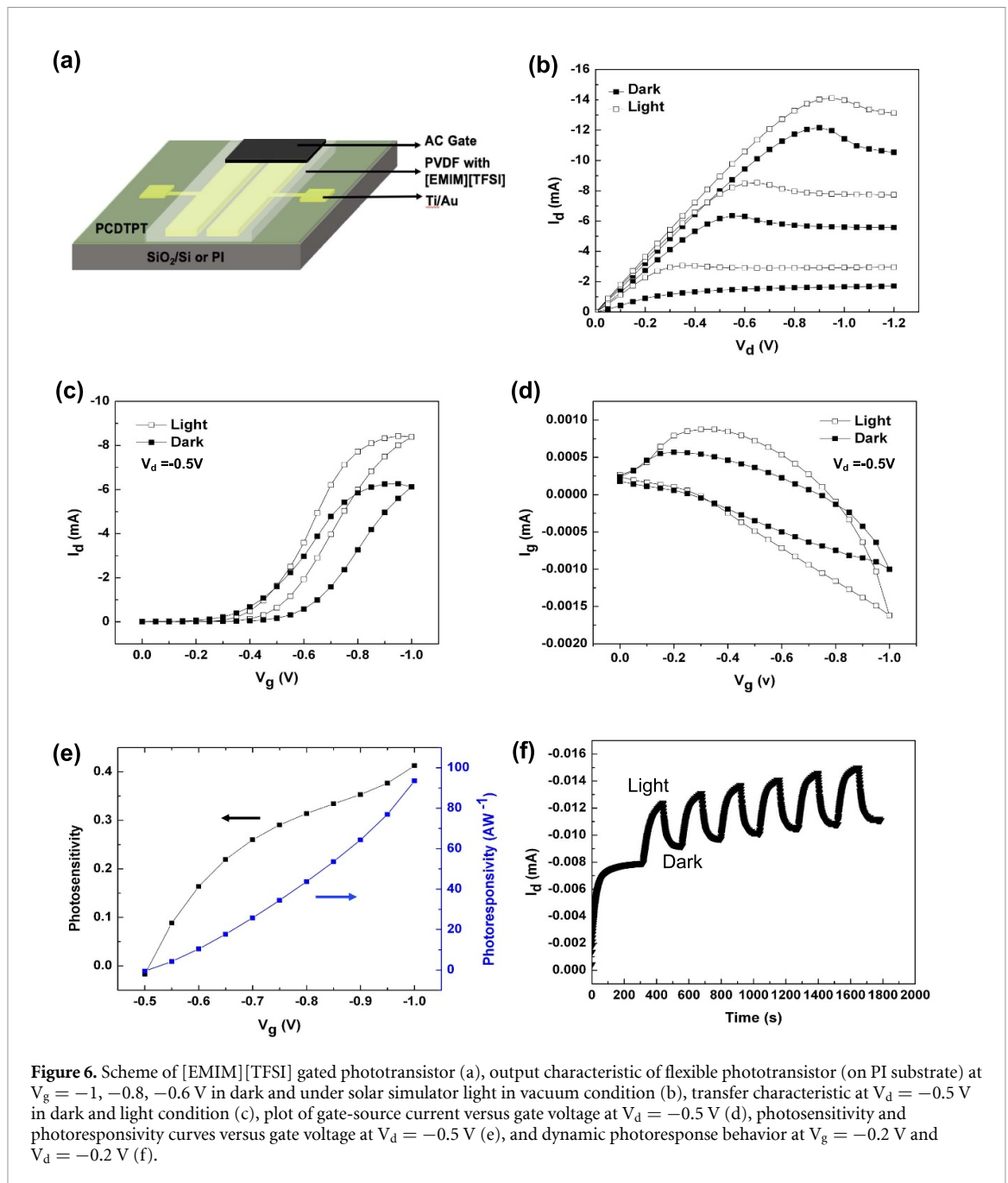

Figure 5. Mobility variation versus different bending curvature (a), Mobility values in different bending cycles with curvature radius of R ∼ 10 mm (b). The error bars represent the standard deviation of the mobility values extracted on 3 devices.

air (figure S5) indicate that the mobility decreases by two orders of magnitude and the threshold voltage increaseas to −0.7 V. After 3 h in ambient air no transistor characteristics could be detected. This can be due to the instability of either PCDTPT or the ionic liquid in ambient air.

We fabricated ion gated transistors on flexible PI substrate, as shown in figure 4(a), and evaluated their performance under different tensile bending conditions (bending of devices was performed with apparatus shown in figure S7). Flat devices (figure 4(b)) show a mobility of 0.86 ± 0.06 cm^2 V^{-1} s^{-1}, very similar to that of rigid devices (repeatability tests for 2 other devices measured under the same conditions is shown in figure S6). A slight decrease in current was observed when the devices were bent perpendicularly to the channel width, with curvature radii $R \sim 20$ mm and $R \sim 10$ mm (figures 4(c) and (d)). Transfer curves in linear and saturation regions were obtained under different bending conditions (figures 4(e) and (f)). The ON–OFF ratio was ∼10^5 for all devices in flat state and bent condition. According to transfer curves in both linear and saturation regime, the current decreased by ∼30% upon bending at $R \sim 10$ mm, with respect to flat devices. Threshold voltages showed a negative shift of ∼20% upon bending up to $R \sim 10$ mm in both linear and saturation regime.

The mobilities at different curvature radii (figure 5(a)) were 0.72 ± 0.04 cm^2 V^{-1} s^{-1} for $R \sim 20$ mm and 0.80 ± 0.03 cm^2 V^{-1} s^{-1} for $R \sim 10$ mm. i.e. almost unchanged with respect to the flat state

Figure 6. Scheme of [EMIM][TFSI] gated phototransistor (a), output characteristic of flexible phototransistor (on PI substrate) at $V_g = -1, -0.8, -0.6$ V in dark and under solar simulator light in vacuum condition (b), transfer characteristic at $V_d = -0.5$ V in dark and light condition (c), plot of gate-source current versus gate voltage at $V_d = -0.5$ V (d), photosensitivity and photoresponsivity curves versus gate voltage at $V_d = -0.5$ V (e), and dynamic photoresponse behavior at $V_g = -0.2$ V and $V_d = -0.2$ V (f).

$(0.86 \pm 0.06$ cm^2 V^{-1} s$^{-1})$. Along with electrical characterization in varied curvature radius we tested the device under repetitive bending cycles. The mobility as a function of the number of bending cycles is shown in figure 5(b). Mobility values in repetitive bending up to 1000 cycles decreased from 0.86 ± 0.06 to 0.68 ± 0.04 cm^2 V^{-1} s^{-1}, i.e. just 20% with respect to the flat state. Optical microscopy images of PCDTPT films after 1000 bending cycles show no significant cracks (figure S8).

In order to evaluate light-sensing application of ion-gated transistors we tested the devices in dark and light conditions. The UV-visible absorption spectrum of a PCDTPT film (figure S9) shows two absorption peaks at 450 and 880 nm. The peak at 450 nm is due to the transition of π-electrons (π–π^*) in bithiophenes and the peak at 880 nm to the charge transfer within a molecule (Wang *et al* 2016). The spectrum shows a lower absorption in the wavelengths of 380 nm–700 nm with respect to other materials such as P3HT (Rahimi *et al* 2014). The scheme of a phototransistor is shown in figure 6(a). The activated carbon gate was placed in a position that was not covering the channel area, so the light could be absorbed by the semiconducting layer. According to output and transfer characterization (figures 6(b) and (c)), the PCDTPT film is photosensitive, i.e. the drain current increases upon irradiation. The atypical shape of the output curves at saturation (figure 6(b)) was observed for several devices measured under vacuum after being fabricated in the glovebox and briefly exposed to air. Although we do not fully understand the origin of this

phenomenon at present, we tentatively attribute it to an ineffective permeation of ions in semiconductor polymer films in vacuum (Panzer and Frisbie 2007), likely due to degradation of the ionic liquid and the semiconductor upon air exposure. The values of charge carrier density in dark and illumination conditions are $(2.19 \pm 0.05) \times 10^{14}$ cm^{-2} and $(2.47 \pm 0.02) \times 10^{14}$ cm^{-2}, respectively (I_g versus V_g curves are shown in figure 6(d)). The mobility increased from 0.78 ± 0.03 cm^2 V^{-1} s^{-1} in the dark to 0.87 ± 0.05 cm^2 V^{-1} s^{-1} under illumination. As these devices were briefly exposed to air before measurements, their mobility values are lower than those of devices tested in glovebox. Phototransistors were evaluated for their photosensitivity $(Ps) = (I_{d,light} - I_{d,dark})/I_{d,dark}$ and photoresponsivity $(R) = (I_{d,light} - I_{d,dark})/p_{light}.S$ and detectivity $(D^*) = RS^{1/2}(2e, I_{d,dark})^{-1/2}$ (Baeg *et al* 2013), where $I_{d,light}$ is the drain-source current in illumination and $I_{d,dark}$ is the drain-source current in the dark, p_{light} is the light intensity and S is the geometrical area of channel (4000 μm $\times$ 10 μm). Photosensitivity and photoresponsivity versus V_g, shown in figure 6(e). The photoresponsivity value increased by factor of ca. 25 by increasing V_g values from -0.5 V to -1 V and reached the value of 93 AW^{-1} at $V_g = -1$ V. This behavior is due to the higher amount of charge carrier accumulation at higher V_g values (Meng 2017). We also obtained the photosensitivity and D^* value of 0.4 and 3.4×10^{10} Jones (cm Hz$^{1/2}$W^{-1}) at $V_g = -1$ V, respectively. Our maximum value of photoresponsivity, (extracted between V_g values of -0.5 V and -1 V) are comparable with phototransistors with planar and vertical field-effect configuration reported by (Zhang *et al* 2019) with operating voltage of -30 V. However, the value of D* is two orders of magnitude lower than the values reported by (Zhang *et al* 2019) which is attributed to higher drain current of ion-gated phototransistors in dark condition (Chow *et al* 2018). Our photosensitivity and photoresponsivity values are lower than those obtained with other organic phototransistors (see table S1), in part because due to the significantly lower operating voltage of our devices (<1 V), in part to the limited light absorption of PCDTPT. The dynamic photosensitivity behavior of ion-gated phototransistors determines their response speed. The transient characteristics (drain current versus pulsed illumination) of a PCDTPT phototransistor are shown in figure 6(f). The measurement was started at $t = 0$ s and after the current (I_d) became stable (at $t = 300$ s) the device was exposed to light. We obtained rise time and fall time from the transient curve. Rise time is defined as the response speed of a phototransistor device under illumination, and as time passed the photocurrent increased from 10% to 90% of maximum value. Fall time is defined as the time needed for the current to decrease from 90% of maximum value to 10% by removing the light source (Han *et al* 2019). We obtained a rise time of $\sim$15 s and a fall time of $\sim$20 s, which are higher compared to values found for phototransistors with OFET configuration (Zhang *et al* 2019), which are $\sim$3 s and 0.05 s. The longer response time of ion-gated phototransistors is due to the slow motion of ions involved in the gating process. (Rawlings *et al* 2019). We also fabricated phototransistor device on SiO$_2$/Si substrate (figure S10), which show similar photosensitivity and photoresponsivity (0.7, 31 AW^{-1}, respectively).

4. Conclusion

We demonstrated fabrication of flexible ion-gated transistor and phototransistor based on donor–acceptor conjugated copolymer (PCDTPT) operating at low voltages (<1 V). Cyclic voltammetry showed that application of ionic liquid ([EMIM][TFSI]) as ion-gating media which is in direct contact with an organic semiconducting layer led to doping/de-doping reactions in a permeable semiconducting copolymer layer. Designed devices on both flexible and rigid substrates exhibited high mobility values. Ion-gated transistors fabricated on PI substrate showed good mechanical flexibility at different curvature radii and repetitive bending cycles. Evaluation of the photosensitivity of flexible ion-gated devices under simulated solar light showed enhancement of charge carrier mobility of devices under illumination. Phototransistors with ion-gated configuration showed photosensitivity of 0.4 and responsivity of 93 AW^{-1}. Development of low-weight flexible transistor with low operating voltages enlightens application of such kinds of devices for novel flexible electronic and optoelectronic devices. On the long-term, flexible ion-gated transistors and phototransistors offer great promises for optical sensor application and bio-inspired imaging systems.

Acknowledgments

ORCID iD

Fabio Cicoira https://orcid.org/0000-0002-0047-608X

References

Allen J B and Larry R F 2001 *Electrochemical Methods Fundamentals and Applications* 2nd (New York: Wiley)

Baeg K J, Binda M, Natali D, Caironi M and Noh Y Y 2013 Organic light detectors: photodiodes and phototransistors *Adv. Mater.* **25** 4267–95

Balakrishna Pillai P, Kumar A, Song X and De Souza M M 2018 Diffusion-controlled faradaic charge storage in high-performance solid electrolyte-gated zinc oxide thin-film transistors *ACS Appl. Mater. Interfaces* **10** 9782–91

Braga D, Erickson N C, Renn M J, Holmes R J and Frisbie C D 2012 High-transconductance organic thin-film electrochemical transistors for driving low-voltage red-green-blue active matrix organic light-emitting devices *Adv. Funct. Mater.* **22** 1623–31

Cho J H, Lee J, Xia Y, Kim B, He Y, Renn M J, Lodge T P and Frisbie C D 2008 Printable ion-gel gate dielectrics for low-voltage polymer thin-film transistors on plastic *Nat. Mater.* **7** 900–6

Chow P C, Matsuhisa N, Zalar P, Koizumi M, Yokota T and Someya T 2018 Dual-gate organic phototransistor with high-gain and linear photoresponse *Nat. Commun.* **9** 1–8

Elgrishi N, Rountree K J, Mccarthy B D, Rountree E S, Eisenhart T T and Dempsey J L 2018 A practical beginner's guide to cyclic voltammetry *J. Chem. Educ.* **95** 197–206

Gao W, Ota H, Kiriya D, Takei K and Javey A 2019 Flexible electronics toward wearable sensing *Acc. Chem. Res.* **52** 523–33

Guo L Q, Han H, Zhu L Q, Guo Y B, Yu F, Ren Z Y, Xiao H, Ge Z Y and Ding J N 2019 Oxide neuromorphic transistors gated by polyvinyl alcohol solid electrolytes with ultralow power consumption *ACS Appl. Mater. Interfaces* **11** 28352–8

Han T, Shou M, Liu L, Xie Z, Ying L, Jiang C, Wang H, Yao M, Deng H and Jin G 2019 Ultrahigh photosensitive organic phototransistors by photoelectric dual control *J. Mater. Chem.* C **7** 4725–32

Huang J, Du J, Cevher Z, Ren Y, Wu X and Chu Y 2017 Printable and flexible phototransistors based on blend of organic semiconductor and biopolymer *Adv. Funct. Mater.* **27** 1604163

Kergoat L, Piro B, Berggren M, Horowitz G and Pham M-C 2012 Advances in organic transistor-based biosensors: from organic electrochemical transistors to electrolyte-gated organic field-effect transistors *Anal. Bioanal. Chem.* **402** 1813–26

Kim J, Hassinen T, Lee W H and Ko S 2017 Fully solution-processed organic thin-film transistors by consecutive roll-to-roll gravure printing *Org. Electron.* **42** 361–6

Kim M, Ha H-J, Yun H-J, You I-K, Baeg K-J, Kim Y-H and Ju B-K 2014 Flexible organic phototransistors based on a combination of printing methods *Org. Electron.* **15** 2677–84

Kim M, Ryu S U, Park S A, Choi K, Kim T, Chung D and Park T 2019 Donor–acceptor-conjugated polymer for high-performance organic field-effect transistors: a progress report *Adv. Funct. Mater.* **30** 1904545

Kyaw A K K, Lay L S, Peng G W, Changyun J and Jie Z 2016 A nanogroove-guided slot-die coating technique for highly ordered polymer films and high-mobility transistors *Chem. Commun.* **52** 358–61

Lamport Z A, Haneef H F, Anand S, Waldrip M and Jurchescu O D 2018 Tutorial: organic field-effect transistors: materials, structure and operation *J. Appl. Phys.* **124** 071101

Lan T, Bélanger F, Soavi F and Santato C 2019 Ambient-stable, ion-gated poly [N-9′-heptadecanyl-2, 7-carbazole-alt-5, 5-(4′, 7′-di-2-thienyl-2′, 1′, 3′-benzothiadiazole)](PCDTBT) transistors and phototransistors *Org. Electron.* **74** 265–8

Lee B H, Hsu B B, Patel S N, Labram J, Luo C, Bazan G C and Heeger A J 2016 Flexible organic transistors with controlled nanomorphology *Nano Lett.* **16** 314–9

Meng X 2017 *Electrolyte-Gated Tungsten Oxide Transistors: Fabrication, Working Mechanism, Device Performance* (École Polytechnique de Montréal Montreal)

Meng X, Quenneville F, Venne F D R, Di Mauro E, Işık D, Barbosa M, Drolet Y, Natile M M, Rochefort D and Soavi F 2015 Electrolyte-gated WO₃ transistors: electrochemistry, structure, and device performance *J. Phys. Chem.* C **119** 21732–8

Meng X, Valitova I, Santato C and Cicoira F 2020 *Tin Oxide Materials* Tin dioxide ion-gated transistors (Amsterdam: Elsevier) 477–488

Nam H J, Cha J, Lee S H, Yoo W J and Jung D-Y 2014 A new mussel-inspired polydopamine phototransistor with high photosensitivity: signal amplification and light-controlled switching properties *Chem. Commun.* **50** 1458–61

Panzer M J and Frisbie C D 2007 Polymer electrolyte-gated organic field-effect transistors: low-voltage, high-current switches for organic electronics and testbeds for probing electrical transport at high charge carrier density *J. Am. Chem. Soc.* **129** 6599–607

Park Y, Jung J W, Kang H, Seth J, Kang Y and Sung M M 2019 Single-crystal poly [4-(4, 4-dihexadecyl-4H-cyclopenta [1, 2-b: 5, 4-b′] dithiophen-2-yl)-alt-[1, 2, 5] thiadiazolo [3, 4-c] pyridine] nanowires with ultrahigh mobility *Nano Lett.* **19** 1028–32

Rahimi K, Botiz I, Agumba J O, Motamen S, Stingelin N and Reiter G 2014 Light absorption of poly (3-hexylthiophene) single crystals *RSC Adv.* **4** 11121–3

Rawlings D, Thomas E M, Segalman R A and Chabinyc M L 2019 Controlling the doping mechanism in poly (3-hexylthiophene) thin-film transistors with polymeric ionic liquid dielectrics *Chem. Mater.* **31** 8820–9

Sadeghi M, Delparastan P, Pierre A and Arias A C 2020 Printed flexible organic transistors with tunable aspect ratios *Adv. Electron. Mater.* **6** 1901207

Silva G V D O, Subramanian A, Meng X, Zhang S, Barbosa M S, Baloukas B, Chartrand D, Gonzáles J C, Orlandi M O and Soavi F 2019 Tungsten oxide ion-gated phototransistors using ionic liquid and aqueous gating media *J. Phys. D: Appl. Phys.* **52** 305102

Son H W, Park J H, Chae M-S, Kim B-H and Kim T G 2020 Bilayer indium gallium zinc oxide electrolyte-gated field-effect transistor for biosensor platform with high reliability *Sensors Actuators* B **312** 127955

Soon C F, Wan Omar W I, Nayan N, Basri H, Narawi M and Kian Sek T 2013 A Bespoke Contact Angle Measurement Software and Experimental Setup for Determination of Surface Tension *4th Int. Conf. on Electrical Engineering and Informatics Universiti Kebangsaan Malaysia.* (https://doi.org/10.1016/j.protcy.2013.12.219)

Subramanian A, George B, Bobbara S R, Valitova I, Ruggeri I, Borghi F, Podestà A, Milani P, Soavi F and Santato C 2020 Ion-gated transistors based on porous and compact TiO₂ films: effect of Li ions in the gating medium *AIP Adv.* **10** 065314

Sun H, Vagin M, Wang S, Crispin X, Forchheimer R, Berggren M and Fabiano S 2018 Complementary logic circuits based on high-performance n-type organic electrochemical transistors *Adv. Mater.* **30** 1704916

Tang H, Kumar P, Zhang S, Yi Z, Crescenzo G D, Santato C, Soavi F and Cicoira F 2015 Conducting polymer transistors making use of activated carbon gate electrodes *ACS Appl. Mater. Interfaces* **7** 969–73

Tartakovsky D M and Dentz M 2019 Diffusion in porous media: phenomena and mechanisms *Transp. Porous Media* **130** 105–27

Tseng H R, Phan H, Luo C, Wang M, Perez L A, Patel S N, Ying L, Kramer E J, Nguyen T Q and Bazan G C 2014 High-mobility field-effect transistors fabricated with macroscopic aligned semiconducting polymers *Adv. Mater.* **26** 2993–8

Valitova I, Kumar P, Meng X, Soavi F, Santato C and Cicoira F 2016 Photolithographically patterned TiO2 films for electrolyte-gated transistors *ACS Appl. Mater. Interfaces* **8** 14855–62

Valitova I, Natile M M, Soavi F, Santato C and Cicoira F 2017 Tin dioxide electrolyte-gated transistors working in depletion and enhancement modes *ACS Appl. Mater. Interfaces* **9** 37013–21

Wang C, Zhang X and Hu W 2020 Organic photodiodes and phototransistors toward infrared detection: materials, devices, and applications *Chem. Soc. Rev.* **49** 653–670

Wang G, Huang K, Liu Z, Du Y, Wang X, Lu H, Zhang G and Qiu L 2018 Flexible, low-voltage, and n-type infrared organic phototransistors with enhanced photosensitivity via interface trapping effect *ACS Appl. Mater. Interfaces* **10** 36177–86

Wang M, Ford M, Phan H, Coughlin J, Nguyen T-Q and Bazan G C 2016 Fluorine substitution influence on benzo [2, 1, 3] thiadiazole based polymers for field-effect transistor applications *Chem. Commun.* **52** 3207–10

Williams R and Goodman A M 1974 Wetting of thin layers of SiO2 by water *Appl. Phys. Lett.* **25** 531–2

Wu X, Lan S, Hu D, Chen Q, Li E, Yan Y, Chen H and Guo T 2019 High performance flexible multilevel optical memory based on a vertical organic field effect transistor with ultrashort channel length *J. Mater. Chem.* C **7** 9229–40

Xia Y, Cho J H, Lee J, Ruden P P and Frisbie C D 2009 Comparison of the mobility–carrier density relation in polymer and single-crystal organic transistors employing vacuum and liquid gate dielectrics *Adv. Mater.* **21** 2174–9

Xu H, Liu J, Zhang J, Zhou G, Luo N and Zhao N 2017a Flexible organic/inorganic hybrid near-infrared photoplethysmogram sensor for cardiovascular monitoring *Adv. Mater.* **29** 1700975

Xu H, Zhu Q, Lv Y, Deng K, Deng Y, Li Q, Qi S, Chen W and Zhang H 2017b Flexible and highly photosensitive electrolyte-gated organic transistors with ionogel/silver nanowire membranes *ACS Appl. Mater. Interfaces* **9** 18134–41

Yan Y, Wu X, Chen Q, Liu Y, Chen H and Guo T 2019 High-performance low-voltage flexible photodetector arrays based on all-solid-state organic electrochemical transistors for photosensing and imaging *ACS Appl. Mater. Interfaces* **11** 20214–24

Ying L, Hsu B B, Zhan H, Welch G C, Zalar P, Perez L A, Kramer E J, Nguyen T-Q, Heeger A J and Wong W-Y 2011 Regioregular pyridal [2, 1, 3] thiadiazole π-conjugated copolymers *J. Am. Chem. Soc.* **133** 18538–41

Yuvaraja S, Nawaz A, Liu Q, Dubal D, Surya S G, Salama K N and Sonar P 2020 Organic field-effect transistor-based flexible sensors *Chem. Soc. Rev.* **49** 3423–3460

Zare Bidoky F, Tang B, Ma R, Jochem K S, Hyun W J, Song D, Koester S J, Lodge T P and Frisbie C D 2020 Sub-3 V ZnO electrolyte-gated transistors and circuits with screen-printed and photo-crosslinked ion gel gate dielectrics: new routes to improved performance *Adv. Funct. Mater.* **30** 1902028

Zhang G, Zhong J, Chen Q, Yan Y, Chen H and Guo T 2019 High-performance organic phototransistors with vertical structure design *IEEE Trans. Electron Devices* **66** 1815–8

Zhang S, Hubis E, Tomasello G, Soliveri G, Kumar P and Cicoira F 2017a Patterning of stretchable organic electrochemical transistors *Chem. Mater.* **29** 3126–32

Zhang Y, Yuan Y and Huang J 2017b Detecting 100 fW cm^{-2} light with trapped electron gated organic phototransistors *Adv. Mater.* **29** 1603969

Zhu Y, Liu G, Xin Z, Fu C, Wan Q and Shan F 2019 Solution-processed, electrolyte-gated In2O3 flexible synaptic transistors for brain-inspired neuromorphic applications *ACS Appl. Mater. Interfaces* **12** 1061–8